Publ. Astron. Soc. Japan **41**, 133–140 (1989)

A Model of Astrophysical Tori with Magnetic Fields

Rika OKADA and Jun FUKUE

Astronomical Institute, Osaka Kyoiku University, Tennoji-ku, Osaka 543

and

Ryoji MATSUMOTO*

Department of Astronomy, Faculty of Science, Kyoto University, Kitashirakawa, Sakyo-ku, Kyoto 606

(Received 1988 August 17; accepted 1988 October 4)

Abstract

A steady axisymmetric model of magnetohydrodynamical tori is constructed under the assumptions that the specific angular momentum is constant in whole space and the magnetic field has only the toroidal component. Furthermore, the gas is assumed to be polytropic and the magnetic field is supposed to be expressed by a power of the density and the radius in some specified manner. The relativistic effect is simulated by use of a pseudo-Newtonian potential. It is found that the configuration of the torus with a toroidal magnetic field is elongated along the symmetry axis because of the dominance by the magnetic field far from the axis. Furthermore, the position of the bottom where the density is maximum approaches the center in comparison with the case without magnetic field, although the shape of the funnel and the location of the cusp do not change. In order for such MHD tori to exist, the values of the parameters, e.g., the specific angular momentum and the Alfvén speed at the bottom are restricted in some ranges.

Key words: Accretion disks; Active galaxies; Astrophysical jets; Astrophysical tori; Magnetohydrodynamics.

1. Introduction

Accretion disks have been well accepted as models of active galactic nuclei, X-ray stars, SS 433, young stellar objects, and so on. Geometrically thin, optically thick standard disks (Shakura and Sunyaev 1973; Novikov and Thorne 1973) have successfully explained the observed spectra in active galactic nuclei (e.g., Malkan 1983) and in low mass X-ray binaries (e.g., Mitsuda et al. 1984).

Geometrically thick disks (accretion tori) have been also extensively examined analytically (Limber 1964; Fishbone and Moncrief 1976; Fishbone 1977; Abramowicz et

* Present address: Department of Information Science, College of Arts and Sciences, Chiba University, Yayoicho, Chiba 260.

al. 1978; Kozłowski et al. 1978; Jaroszyński et al. 1980; Paczyński and Wiita 1980), and numerically (Hawley et al. 1984; Hawley 1986; Robertson and Frank 1986; Kuwahara 1988). Such a geometrically thick configuration will be realized in the case where the accretion rate exceeds the critical rate and hence the radiation pressure supports the torus (Abramowicz et al. 1978; Kozłowski et al. 1978) or in the case that the accretion rate is so low and the ion pressure supports the gas (Rees et al. 1982). The geometrically thick torus is astrophysically important, since such a torus is suggested to be responsible for astrophysical jets in various astronomical objects (Lynden-Bell 1978; Fukue 1982, 1983).

In a gaseous torus differentially rotating around a central object, the toroidal magnetic field will be easily generated by differential rotation, if there is a seed poloidal field frozen in the accreting matter. Until now, however, little attention is focused on the geometrically thick torus with magnetic field.

In this paper we examine the structure of magnetized tori under the magnetohydrodynamical treatment. The configuration of the torus is modified by the toroidal magnetic field.

In the next section the basic equations and assumptions are presented. Typical structures of MHD tori are shown in section 3. The final section is devoted to discussion.

2. Basic Equations

Let us consider the stationary, axisymmetric tori surrounding the central object of mass M. As the gravitational potential of the central object, in order to mimic the relativistic effect, we use the pseudo-Newtonian potential (Paczyński and Wiita 1980):

$$\phi=-\frac{GM}{r-r_{\rm g}}, \tag{1}$$

where $r=(\varpi^2+z^2)^{1/2}$ is the distance from the center and $r_{\rm g}=2GM/c^2$ is the Schwarzschild radius of the central object. Here and hereafter, we adopt the cylindrical coordinates (ϖ, φ, z), where the z-axis is coincident with the rotation axis of the tori.

We assume that the gas of the tori has no motion in the meridional plane and the specific angular momentum is constant in the whole space, although it is straightforward to extend the present treatment to any given distribution of angular momentum. We neglect the self-gravity of the gas and assume that the gas is inviscid and adiabatic. The tori are further assumed to have only the toroidal component of the magnetic field, B_φ.

Under the above assumptions, the basic equations governing the structure of the magnetized torus are described as follows. First the equations of motion are

$$\frac{\partial\phi}{\partial\varpi}-\frac{L^2}{\varpi^3}+\frac{1}{\rho}\frac{\partial p}{\partial\varpi}=-\frac{B_\varphi}{4\pi\varpi\rho}\frac{\partial}{\partial\varpi}(\varpi B_\varphi), \tag{2}$$

$$\frac{\partial\phi}{\partial z}+\frac{1}{\rho}\frac{\partial p}{\partial z}=-\frac{B_\varphi}{4\pi\rho}\frac{\partial B_\varphi}{\partial z}, \tag{3}$$

where L is the specific angular momentum of the torus gas, ρ the gas density, and p the gas pressure.

We use the polytropic relation as the equation of state:

$$p = K\rho^{\gamma}, \tag{4}$$

where K and γ are constants.

As for the magnetic field, in order to treat the problem analytically, we impose the assumption that the Alfvén speed c_A is a function of ϖB_φ. In particular, we assume the form

$$c_A{}^2 \equiv \frac{B_\varphi{}^2}{4\pi\rho} = \frac{(4\pi H)^{1/\mu}}{4\pi}(\varpi B_\varphi)^{2(\mu-1)/\mu}, \tag{5}$$

where H and μ are assumed to be constants. We note that the Alfvén speed is constant when $\mu = 1$.

In what follows, we shall take the Schwarzschild radius r_g and the light speed c as the units of length and velocity, respectively. Hence, e.g., the unit of potential is c^2.

Using equations (4) and (5), we can integrate equations (2) and (3) into the potential form

$$\psi = -\frac{1}{2(r-1)} + \frac{L^2}{2\varpi^2} + \frac{1}{\gamma-1}c_s{}^2 + \frac{\mu}{2(\mu-1)}c_A{}^2 = \psi_0 \text{ (constant)}, \tag{6}$$

where the square of the sound speed and the square of the Alfvén speed are respectively written as

$$c_s{}^2 = K\gamma\rho^{\gamma-1}, \tag{7}$$

$$c_A{}^2 = H\varpi^{2(\mu-1)}\rho^{\mu-1}. \tag{8}$$

The constant ψ_0 is the value of the potential ψ at the surface of the torus where $\rho = 0$.

For convenience sake, we shall rewrite the Alfvén speed in equation (6) in terms of the sound speed and the quantities at the torus bottom, which is defined as a position where the sound speed is maximum. After some manipulations, we have

$$\psi = -\frac{1}{2(r-1)} + \frac{L^2}{2\varpi^2} + \frac{1}{\gamma-1}c_s{}^2 + \frac{\mu}{2(\mu-1)}\frac{c_{Ab}^2}{\varpi_b^{2(\mu-1)}c_{sb}^{2(\mu-1)/(\gamma-1)}}\varpi^{2(\mu-1)}c_s^{2(\mu-1)/(\gamma-1)}, \tag{9}$$

where c_{Ab} is the Alfvén speed at the bottom of the torus. The radius of the bottom ϖ_b is obtained as a root of the equation:

$$\frac{1}{2(\varpi_b-1)^2} - \frac{L^2}{\varpi_b{}^3} + \frac{\mu c_{Ab}^2}{\varpi_b} = 0. \tag{10}$$

Moreover, the sound speed at the bottom c_{sb} is expressed as

$$c_{sb}^2 = (\gamma-1)\left[\psi_0 + \frac{1}{2(\varpi_b-1)} - \frac{L^2}{2\varpi_b{}^2} - \frac{\mu c_{Ab}^2}{2(\mu-1)}\right]. \tag{11}$$

Ultimately, the parameters describing the structure of MHD tori in the present model are γ, μ, L, ψ_0, and c_{Ab}. In the next section, we shall fix γ, μ, L, and ψ_0, and examine the effect of the magnetic field on the structure of the tori through c_{Ab}.

3. MHD Torus

The meridional configurations of the (MHD) tori in the present model are shown in figures 1 and 2. The abscissas in these figures are the radius ϖ, while the ordinates are the height z, both being in units of the Schwarzschild radius. The parameters are fixed as $\gamma = 5/3$, $\mu = 5/3$, $L = 2$, and $\psi_0 = 0$.

Figure 1 shows the configuration of the usual gaseous torus without magnetic field (e.g., Limber 1964; Abramowicz et al. 1978; Kozłowski et al. 1978). The contours plotted in the figure represent the levels of isosound speed and are shown in equal steps. From the polytropic assumption, these are parallel to the isodensity contours. As is well known, due to the centrifugal barrier, a funnel is formed along the rotation axis of the torus and it is suggested that the funnel is responsible for the confinement and acceleration of the astrophysical jets (Lynden-Bell 1978; Sikora and Wilson 1981; Fukue 1982, 1983; Calvani and Nobili 1983). Far from the rotation axis, the contours are approximately spherical.

On the other hand, figure 2 shows the typical configuration of the torus with the toroidal magnetic field in the specified manner expressed by equation (5). In this example, the Alfvén speed at the bottom is $c_{Ab} = 0.1$. Hence, from equations (10) and (11), the sound speed at the bottom is $c_{sb} = 0.14$ and the bottom is located at $\varpi_b = 4.39$. It is worthwhile noting that the ratio of the magnetic pressure to the gas pressure at the bottom, $\alpha = c_{Ab}^2/2c_{sb}^2$, is 0.24.

Comparing figures 1 and 2, we can easily see that the contours of the MHD tori

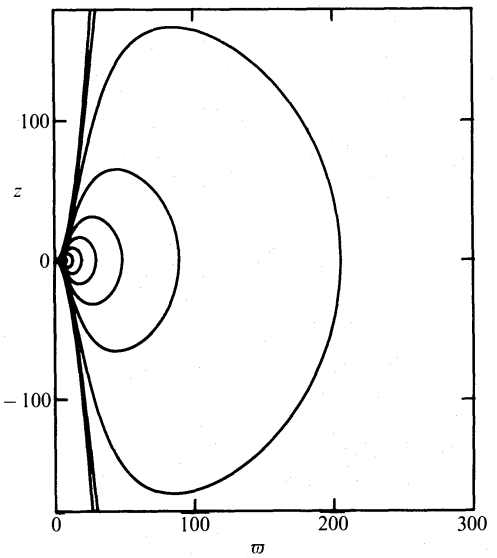

Fig. 1. Typical configuration of a gaseous torus in the meridional plane with a constant specific angular momentum L and without magnetic field. The abscissa is the radius and the ordinate is the height. The contours represent the isosound speed levels which are parallel to the isodensity levels. The parameters are fixed as $\gamma = 5/3$, $L = 2$, and $\psi_0 = 0$.

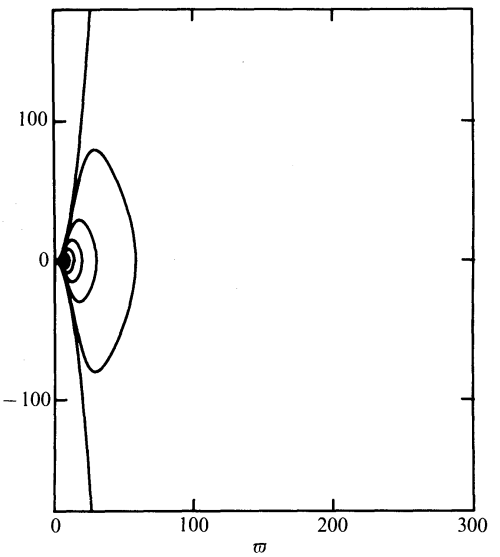

Fig. 2. Typical configuration of an MHD torus in the meridional plane with a constant specific angular momentum and with toroidal magnetic field. The Alfvén speed at the bottom is set as $c_{Ab} = 0.1$ in this example. The other parameters are fixed as $\gamma = 5/3$, $\mu = 5/3$, $L = 2$, and $\psi_0 = 0$.

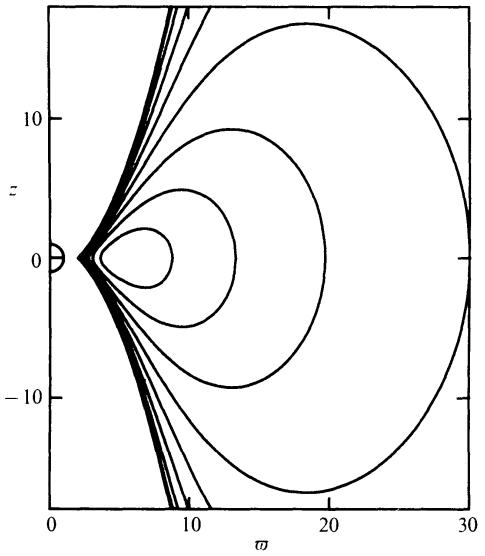

Fig. 3. The central region of figure 1. The cusp is located at $\varpi=2$, whereas the bottom is located at $\varpi=5.24$.

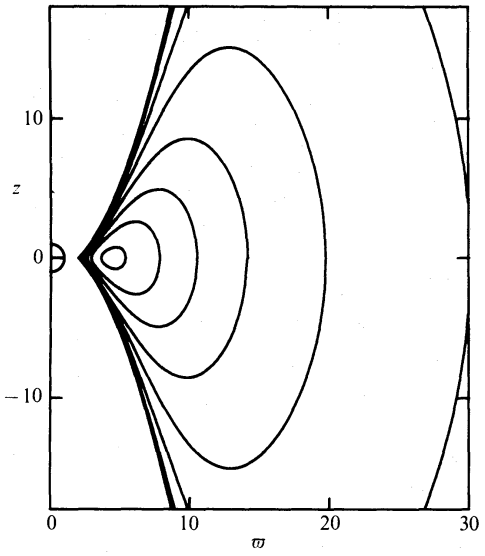

Fig. 4. The central region of figure 2. The shape and the location of the cusp are the same as that of the tori without magnetic field shown in figure 3. The bottom, however, is located at $\varpi=4.39$ and approaches the center in comparison with that of the gaseous torus without magnetic field.

are remarkably elongated in the vertical direction (or compressed in the radial direction) in the outer region. Hence the isosound speed (isodensity) contours in the outer region become prolate spheroids. This is because the supposed toroidal magnetic field pinches the gas, and because the gas in the torus (especially, in the outer region) is removed by the magnetic pressure. These elongated configurations of the MHD torus are of use for confining the astrophysical jets accelerating in the funnel.

In the vicinity of the rotation axis, the shapes of the surfaces of the tori and the positions of the cusp, where the effective potential is locally maximum and the isopotential contour crosses itself, are not altered. These are demonstrated in figures 3 and 4, where the central regions of figures 1 and 2 are shown, respectively.

This is because on the surface of the torus where the gas density becomes zero the magnetic field also vanishes from the assumption (5). The location of the bottom, however, approaches the center when the toroidal magnetic field is taken into consideration. This point will be discussed in the next section.

4. Discussion

In the present paper, we show a specific model of MHD tori where the gas is circularly rotating around the central object and the toroidal magnetic field in the torus has some specific form. In this section, we shall discuss several restrictions imposed on the present model.

4.1. Parameter Ranges

In the present model there are several parameters: γ, μ, L, ψ_0, and c_{Ab}. Of these, the

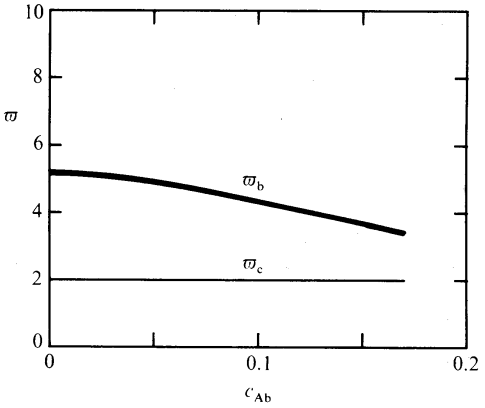

Fig. 5. The location of the bottom as a function of the Alfvén speed at the bottom (thick solid curve). The locus of the cusp is also plotted by the thin solid curve. The other parameters are fixed as $\gamma=5/3$, $\mu=5/3$, $L=2$, and $\psi_0=0$.

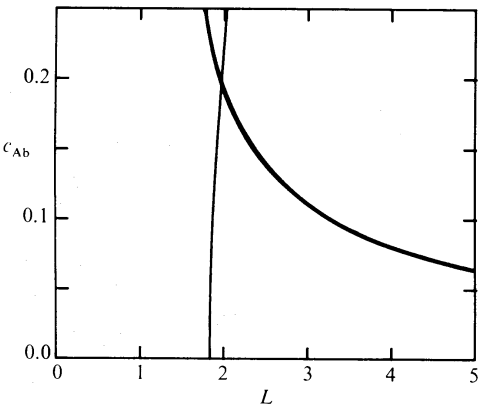

Fig. 6. The permitted region for the parameters L and c_{Ab}. The other parameters are fixed as $\gamma=5/3$, $\mu=5/3$, and $\psi_0=0$. Above the thick solid curve, the magnetic pressure becomes so strong that all the gas in the torus is excluded. On the left of the almost vertical thin curve, the angular momentum is so small that the cusp and the bottom merge together.

influence of the magnetic field on the structure of the tori is manifested through the Alfvén speed at the bottom c_{Ab}. As was mentioned, if this Alfvén speed at the bottom becomes larger, the position of the bottom approaches more closely the center. In figure 5, the location of the bottom on the equator is plotted as a function of the Alfvén speed at the bottom by the thick solid curve. The thin solid curve denotes the locus of the cusp which does not depend on c_{Ab}. The other parameters are fixed as $\gamma=5/3$, $\mu=5/3$, $L=2$, and $\psi_0=0$.

The curves in figure 5 are terminated at about $c_{Ab}=0.17$. Beyond some critical value of c_{Ab}, MHD tori cannot exist, either because the sound speed at the bottom determined by equation (11) is negative, or because the magnetic pressure becomes so large that all the gas in the torus is excluded.

Figure 6 shows the region of the parameter range where the MHD tori of the present model exist. The abscissa of figure 6 is the specific angular momentum L and the ordinate is the Alfvén speed at the bottom c_{Ab}. The other parameters are fixed as $\gamma=5/3$, $\mu=5/3$, and $\psi_0=0$.

For a given L, there exists a maximum value of c_{Ab}, beyond which the present torus does not exist, since the sound speed at the bottom is negative. This constraint is shown by the thick solid curve. On the other hand, the thin solid curve represents another constraint; that is, on the left of this curve, the angular momentum is so small that the cusp and the bottom merge and the gas cannot accumulate in the potential well. Although this curve is almost vertical and the dependence on c_{Ab} is weak, the minimum value of the specific angular momentum slightly increases as the Alfvén speed at the bottom increases.

4.2. *Effective Polytropic Index*

Using equations (7) and (8), for $\gamma=\mu$, we can express the third and fourth terms on

the right-hand side of equation (6) in the form

$$\frac{c_s{}^2}{\Gamma-1}, \tag{12}$$

where the effective polytropic index is

$$\Gamma=\frac{\gamma+(H/2K)\varpi^{2(\gamma-1)}}{1+(H/2K)\varpi^{2(\gamma-1)}}. \tag{13}$$

As seen from equation (13), $\Gamma\sim\gamma$ and the configuration of the MHD tori resembles that without magnetic field when H/K is negligible or the radius is small. On the other hand, Γ approaches unity and the configuration of MHD tori resembles that of an isothermal gas for large ϖ. This means that the magnetic pinch effect works so as to reduce the effective polytropic index.

4.3. Remarks

The crucial assumption of the present MHD tori is equation (5), which relates the magnetic field to the gas density so that the equations of motion are integrable. This relation (5) is analogous to the polytropic relation for the gas, although there seems to be no physical meaning in equation (5) unlike the polytropic relation. However, we should mention again that there is a more general relation analogous to the barotropic relation. That is to say, the equations of motion (2) and (3) are integrated into the potential form, if c_A^2 is a function of ϖB_φ. The present case is a special one where the function is a power function. Qualitative properties of the configuration of the MHD tori in a more general case, however, will not much differ from the present simple case.

There is another severe problem, i.e., instability. It is supposed that differentially rotating gaseous tori are in general dynamically unstable (Hacyan 1982; Papaloizou and Pringle 1984) against nonaxisymmetric perturbations. However, it is considered that the reflecting boundaries are necessary in order for the instability to increase (Kato 1987). Moreover, accretion flows are also supposed to suppress instability (Blaes 1987). Therefore, it is an open question at the present stage that such a dynamical instability operates in realistic astrophysical tori.

If the magnetic field is included, the situation becomes more complicated. There appears another mode of instability such as magnetic buoyancy instability (Parker 1979; Acheson 1979; Horiuchi et al. 1988; Matsumoto et al. 1988). The study of the instability problem for the present MHD tori remains to be carried out in the future.

The authors would like to thank Professor S. Kato and Dr. H. Itoh for useful comments and discussions. This work was supported in part by a Grant-in-Aid for Scientific Research of the Ministry of Education, Science, and Culture (62740145, 63740133).

References

Abramowicz, M., Jaroszyński, M., and Sikora, M. 1978, *Astron. Astrophys.*, **63**, 221.
Acheson, B. J. 1979, *Solar Phys.*, **62**, 23.
Blaes, O. M. 1987, *Monthly Notices Roy. Astron. Soc.*, **227**, 975.

Calvani, M., and Nobili, L. 1983, in *Astrophysical Jets*, ed. A. Ferrari and A. G. Pacholczyk (D. Reidel Publishing Company, Dordrecht), p. 189.
Fishbone, L. G. 1977, *Astrophys. J.*, **215**, 323.
Fishbone, L. G., and Moncrief, V. 1976, *Astrophys. J.*, **207**, 962.
Fukue, J. 1982, *Publ. Astron. Soc. Japan*, **34**, 163.
Fukue, J. 1983, *Publ. Astron. Soc. Japan*, **35**, 539.
Hacyan, S. 1982, *Astrophys. J.*, **262**, 322.
Hawley, J. F. 1986, in *Radiation Hydrodynamics in Stars and Compact Objects*, ed. D. Mihalas and K.-H. A. Winkler (Springer-Verlag, Berlin), p. 369.
Hawley, J. F., Smarr, L. L., and Wilson, J. R. 1984, *Astrophys. J. Suppl.*, **55**, 211.
Horiuchi, T., Matsumoto, R., Hanawa, T., and Shibata, K. 1988, *Publ. Astron. Soc. Japan*, **40**, 147.
Jaroszyński, M., Abramowicz, M. A., and Paczyński, B. 1980, *Acta Astron.*, **30**, 1.
Kato, S. 1987, *Publ. Astron. Soc. Japan*, **39**, 645.
Kozłowski, M., Jaroszyński, M., and Abramowicz, M. A. 1978, *Astron. Astrophys.*, **63**, 209.
Kuwahara, F. 1988, submitted to *Prog. Theor. Phys.*
Limber, D. N. 1964, *Astrophys. J.*, **140**, 1391.
Lynden-Bell, D. 1978, *Phys. Scr.*, **17**, 185.
Malkan, M. A. 1983, *Astrophys. J.*, **268**, 582.
Matsumoto, R., Horiuchi, T., Shibata, K., and Hanawa, T. 1988, *Publ. Astron. Soc. Japan*, **40**, 171.
Mitsuda, K., Inoue, H., Koyama, K., Makishima, K., Matsuoka, M., Ogawara, Y., Shibazaki, N., Suzuki, K., Tanaka, Y., and Hirano, T. 1984, *Publ. Astron. Soc. Japan*, **36**, 741.
Novikov, I. D., and Thorne, K. S. 1973, in *Black Holes*, ed. C. DeWitt and B. S. DeWitt (Gordon and Breach, New York), p. 343.
Paczyński, B., and Wiita, P. J. 1980. *Astron. Astrophys.*, **88**, 23.
Papaloizou, J. C. B., and Pringle, J. E. 1984, *Monthly Notices Roy. Astron. Soc.*, **208**, 721.
Parker, E. N. 1979, *Cosmical Magnetic Fields* (Clarendon Press, Oxford), p. 314.
Rees, M. J., Begelman, M. C., Blandford, R. D., and Phinney, E. S. 1982, *Nature*, **295**, 17.
Robertson, J. A., and Frank, J. 1986, *Monthly Notices Roy. Astron. Soc.*, **221**, 279.
Shakura, N. I., and Sunyaev, R. A. 1973, *Astron. Astrophys.*, **24**, 337.
Sikora, M., and Wilson, D. B. 1981, *Monthly Notices Roy. Astron. Soc.*, **197**, 529.